

# NAVAL POSTGRADUATE SCHOOL

## Monterey, California



IMPULSIVE FLOW ABOUT A CIRCULAR CYLINDER

By

TURGUT SARPKAYA

March 1978

Approved for public release; distribution unlimited.

Feadoes

D 208, 14/2.

NFS-695L-78-008

NAVAL POSTGRADUATE SCHOOL  
Monterey, California

Rear Admiral T. F. Dedman  
Superintendent

Jack R. Borsting  
Provost

The work reported herein was supported by the National Science Foundation, Washington, D. C. 20550, through Grant No. ENG76-24584.

Reproduction of all or part of this report is authorized.

This report was prepared by:



REPORT DOCUMENTATION PAGE		READ INSTRUCTIONS BEFORE COMPLETING FORM
1. REPORT NUMBER NPS-69SL-78-008	2. GOVT ACCESSION NO.	3. RECIPIENT'S CATALOG NUMBER
4. TITLE (and Subtitle) IMPULSIVE FLOW ABOUT A CIRCULAR CYLINDER		5. TYPE OF REPORT & PERIOD COVERED Interim, 3/77 to 3/78
		6. PERFORMING ORG. REPORT NUMBER
7. AUTHOR(s) Turgut Sarpkaya		8. CONTRACT OR GRANT NUMBER(s) Grant No. ENG76-24584
9. PERFORMING ORGANIZATION NAME AND ADDRESS Naval Postgraduate School Monterey, California 93940		10. PROGRAM ELEMENT, PROJECT, TASK AREA & WORK UNIT NUMBERS
11. CONTROLLING OFFICE NAME AND ADDRESS National Science Foundation Fluid Mechanics Program Washington, D. C. 20550		12. REPORT DATE March 1978
		13. NUMBER OF PAGES 37
14. MONITORING AGENCY NAME & ADDRESS (if different from Controlling Office)		15. SECURITY CLASS. (of this report)
		15a. DECLASSIFICATION/DOWNGRADING SCHEDULE
16. DISTRIBUTION STATEMENT (of this Report) Approved for public release; distribution unlimited. Reproduction in whole or in part is permitted for any purpose of the United States Government.		
17. DISTRIBUTION STATEMENT (of the abstract entered in Block 20, if different from Report)		
18. SUPPLEMENTARY NOTES		
19. KEY WORDS (Continue on reverse side if necessary and identify by block number) Impulsive flow, cross-flow analogy		
20. ABSTRACT (Continue on reverse side if necessary and identify by block number) The drag and lift forces acting on smooth circular cylinders in an impulsively-started flow have been measured through the use of a vertical water tunnel. The drag and lift coefficients were found to depend on the Reynolds number and the normalized displacement of the fluid from the start. It is recommended that these experiments be extended to higher Reynolds numbers to substantiate further the Reynolds number dependence.		



# Impulsive Flow About a Circular Cylinder

Turgut Sarpkaya

## ABSTRACT

The drag and lift forces acting on smooth circular cylinders in an impulsively-started flow have been measured through the use of a vertical water tunnel.

The drag and lift coefficients were found to depend on the Reynolds number and the normalized displacement of the fluid from the start.

It is recommended that these experiments be extended to higher Reynolds numbers to substantiate further the Reynolds number dependence.





## TABLE OF CONTENTS

I.	INTRODUCTION - - - - -	9
II.	PREVIOUS STUDIES AND THE IMPULSIVE FLOW ANALOGY - - - - -	10
III.	EXPERIMENTAL ARRANGEMENT - - - - -	14
	A. TEST FACILITY - - - - -	14
	B. ACCELERATION AND VELOCITY MEASUREMENTS - - - - -	14
	C. TEST BODIES AND FORCE MEASUREMENT - - - - -	17
IV.	DISCUSSION OF RESULTS - - - - -	19
	A. DRAG COEFFICIENT - - - - -	19
	B. LIFT COEFFICIENT - - - - -	27
V.	CONCLUSIONS - - - - -	34
	LIST OF REFERENCES - - - - -	35
	INITIAL DISTRIBUTION LIST - - - - -	37



## LIST OF FIGURES

### Figure

1. Symmetric vortex separation on a slender body of revolution at high angle of attack, NACA model	11
2. Schematic drawing of the vertical water tunnel	15
3. Valve assembly	16
4. $C_D$ vs $Ut/c$ for Reynolds numbers 15,350, 16,200, and 16,650	20
5. $C_D$ vs $Ut/c$ for Reynolds numbers 20,300 and 20,700	21
6. $C_D$ vs $Ut/c$ for Reynolds numbers 32,000, 32,600, and 33,200	22
7. $C_D$ vs $Ut/c$ for Reynolds numbers 32,900 and 32,800 (two runs)	23
8. $C_D$ vs $Ut/c$ for Reynolds numbers 33,600 and 34,000 (two runs)	24
9. $C_L$ vs $Ut/c$ for Reynolds numbers 20,600, 22,100, and 21,700 (two runs)	28
10. $C_L$ vs $Ut/c$ for Reynolds number 32,600 (two runs)	29
11. $C_L$ vs $Ut/c$ for Reynolds number 34,100 (three runs)	30
12. $C_L$ vs $Ut/c$ for Reynolds numbers 34,800 and 34,900	31



## NOMENCLATURE

$c$	Radius of the test cylinder
$C_D$	Drag coefficient
$C_L$	Lift coefficient
$D$	Diameter of the test cylinder
$\ell$	Distance between pressure taps of accelerometer
$L$	Length of the test cylinder
$p$	pressure
$\Delta p$	differential pressure
$Re$	Reynolds number
$t$	Time
$U$	Velocity
$\frac{dU}{dt}$	Acceleration
$\Gamma$	Circulation
$\nu$	Fluid kinematic viscosity
$\rho$	Fluid density



## ACKNOWLEDGMENTS

The work described in this report represents part of a research program supported by the Engineering Division of the National Science Foundation. This support is gratefully acknowledged.

The writer is indebted to the many people whose co-operation made this investigation possible. Messrs. Ray L. Shoaff and Wolfgang M. S. Bruns, graduate students at the Naval Postgraduate School, assisted with the experiments and data evaluation. Mr. Jack McKay built all the critical parts of the instrumentation.





## 1. INTRODUCTION

The understanding of the kinematics and dynamics of the impulsively started flow about bluff bodies in general and a circular cylinder in particular is of both practical and fundamental importance. From a theoretical point of view, analytical and experimental results enable one to understand the evolution of the separation of flow and the symmetric vortex development.

From a practical point of view, the understanding of the characteristics of impulsive flow enables one to calculate the normal and side forces acting on slender bodies of revolution at large angles of attack through the use of the so-called "impulsive flow analogy".

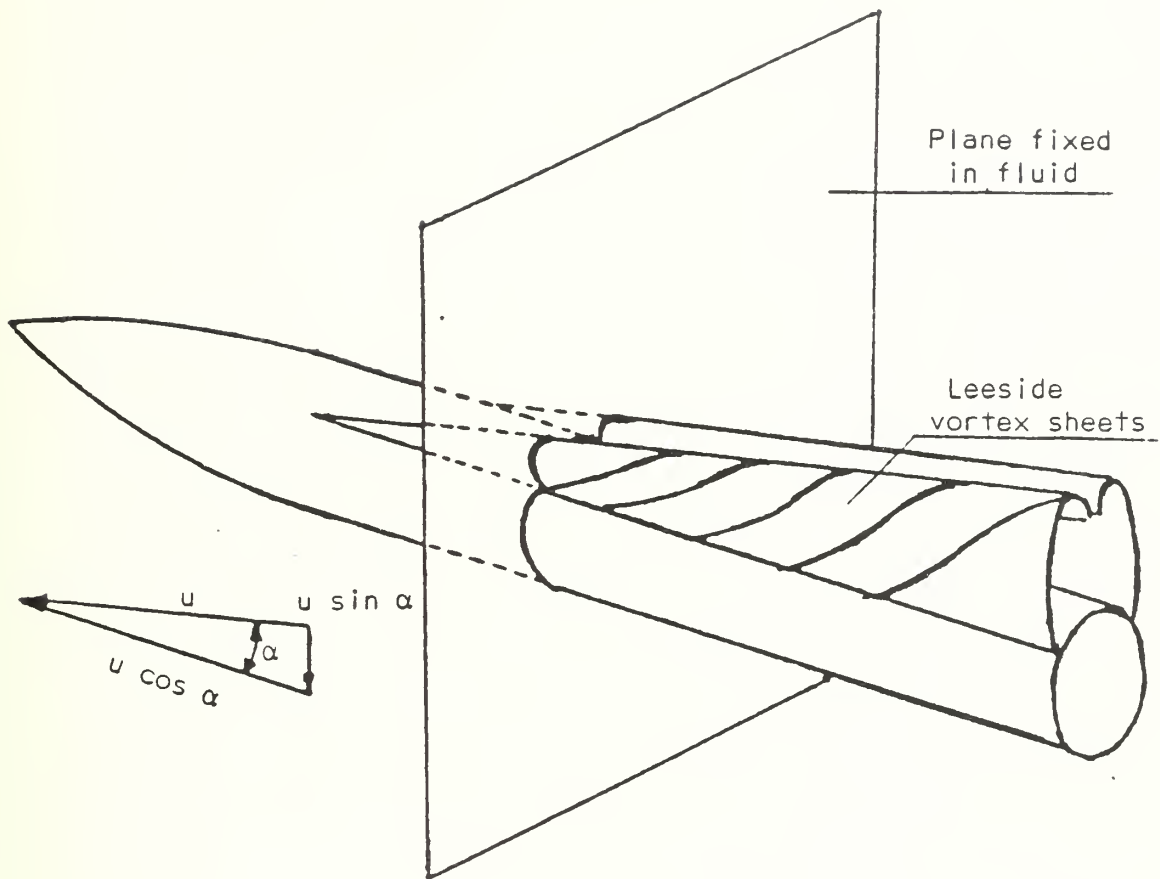
The present investigation addressed itself to the experimental determination of the drag (normal) force and lift (side) force acting on smooth cylinders immersed in an impulsively started flow through the use of a vertical water tunnel.



## 11. PREVIOUS STUDIES AND THE IMPULSIVE FLOW ANALOGY

When a slender body is inclined to a flow, it experiences a component of force in the plane in which the inclination occurs and a component perpendicular to that plane. These forces will be referred to hereafter as drag and lift forces. Earlier works were mainly concerned with the drag forces at moderate angles of attack. The flow pattern at small to moderate angles of attack consists of a pair of axially oriented symmetric vortices on the lee side of the lifting body. This physical flow field was approximated by the so-called NACA vortex model (See Fig. 1). Munk [1] was one of the first to study the problem and to introduce the cross-flow approach, which has been the basis of all drag-force prediction methods. Munk's work was primarily concerned with an ideal fluid and only relevant to small angles of inclination. Allen and Perkins [2] considered slender bodies at large angles of inclination, where the viscous effects and separation are important, and modelled the cross-flow development by analogy with the flow over an impulsively started cylinder. In other words, they have hypothesized that the evolution of the spiralling vortex sheets with distance along a slender body is similar to the evolution of symmetric vortices with time in an impulsively-started flow about a circular cylinder. This hypothesis turned out to be a very fruitful one and has been developed by later workers; for example Sarpkaya [3], Kelly [4], Hill [5], and Bryson [6] devised various approximate discrete-vortex models to study the evolution of vortices behind an impulsively started cylinder.





• Figure 1. Symmetric vortex separation on a slender body of revolution at high angle of attack, NACA model.



These models were able to predict in an approximate way only the early stages of motion. These investigators were not concerned with the development of asymmetry in the wake and subsequent vortex shedding.

Vortices peel off from missiles flying at high angles of attack and give rise to significant side or lift forces. In spite of the realization of the need for theoretical analysis and experimental data either for side forces acting on missiles or for lift forces acting on cylinders in impulsively started flow, there has been practically no data or systematic study.

The development of flow about a cylinder started impulsively from rest was first studied by Blasius [7]. He has shown that the flow about the cylinder does not begin to separate until a distance of  $s = 0.351 c$  is covered by the flow. Blasius' work has later been extended by Goldstein and Rosenhead [8], Görtler [9], Schuh [10], Watson [11], and Wundt [12]. They have demonstrated that the separation depends on the shape of the body, the Reynolds number, and the particular time dependence of flow from the start of motion. Following the inception of separation at the rear stagnation point, the separation points move rapidly around the body until at large values of time they reach a nearly steady state position, often quite close to that observed experimentally in steady flow about the same body.

In spite of its relevance to the impulsive-flow analogy, relatively little experimental work has been carried out on impulsively started flow about cylinders. Schwabe [13] dragged a cylinder of 9 cm diameter in a shallow channel at a speed of 0.8 cm/sec through the use of weights and pulleys and attained Reynolds numbers of about 600. He developed a procedure which enabled him to calculate pressure





distribution and hence the drag force from the pictures of the flow pattern. Schwabe's drag coefficient is about twice as large as the steady state value and is still increasing after the cylinder has displaced a distance of about 9 body radii. Approximate numerical analysis carried out by Bryson [6] shows a maximum of about 1.5 for the drag coefficient at the time when the cylinder moved about 4 body radii. Subsequently, the drag coefficient drops to an unrealistically low value as noted by Bryson.

The only other investigation in recent times was undertaken by Sarpkaya [3] through the use of a vertical water tunnel. He found that the drag coefficient reaches a value of about 1.5 at a relative fluid displacement of about 8 body radii. In spite of the difficulties encountered by him in generating an impulsively-started flow, his results have clearly shown that the drag coefficient does reach a maximum of about 1.5 and then rapidly decreases to a steady state value of about 1.2. The method developed by him has been further improved and utilized in the present investigation not only for the purpose of more accurately determining the exact position of the maximum drag coefficient but also the evolution of the lift coefficient. Consequently, the work described herein presents drag force data which may be compared with those obtained previously and also lift force data for which there is no previous work.



### III. EXPERIMENTAL ARRANGEMENT

#### A. TEST FACILITY

The experiments described herein were conducted in a vertical water tunnel designed by Professor T. Sarpkaya (See Fig. 2). A quick release valve mechanism which opened or closed with the help of a three-way valve was mounted at the bottom of the tunnel. When the quick release valve was opened, the fluid (water) moved downward through the tunnel into an underground reservoir. The particular valve design is shown in Fig. 3. It allows an initial drop within a very short time period and then a slow further opening. The rate of initial drop as well as that of the subsequent valve motion is controlled by a piston in the lower part of the valve and the viscosity of oil in the liquid chamber. The amount of the initial drop, the area of the opening between the liquid chamber and the upper air chamber as well as the viscosity of the oil are variable and easily adjusted to obtain constant velocities at desired rates. Suffice it to note that the system was capable of producing an impulsively started steady flow with very little initial disturbances at desired velocities. In fact the acceleration of the flow was confined to a time period of about 0.05 sec for steady flow velocities of about 40 cm/sec.

#### B. ACCELERATION AND VELOCITY MEASUREMENTS

The acceleration of the fluid was monitored by means of a differential-pressure transducer connected to two pressure taps along a



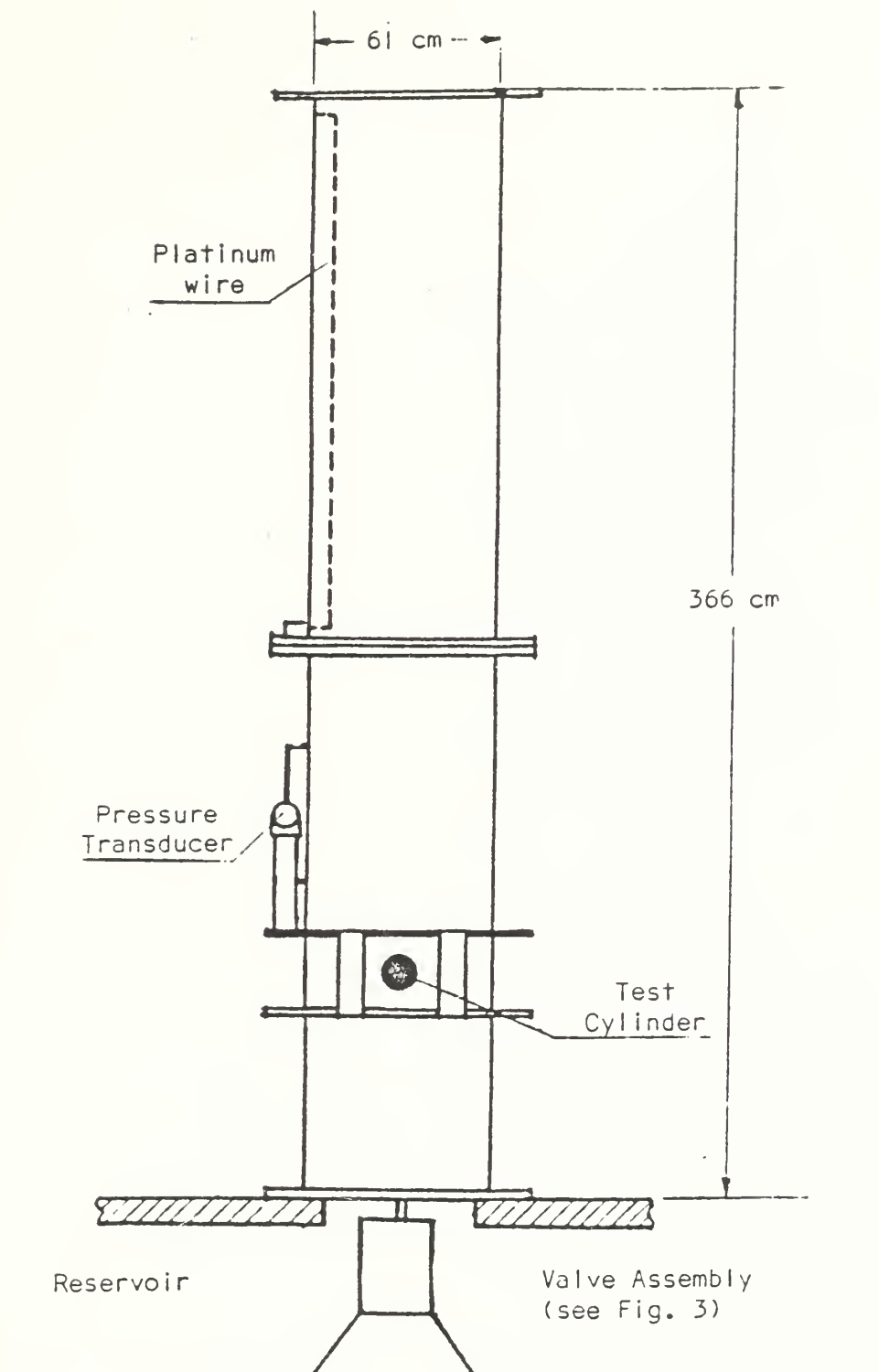
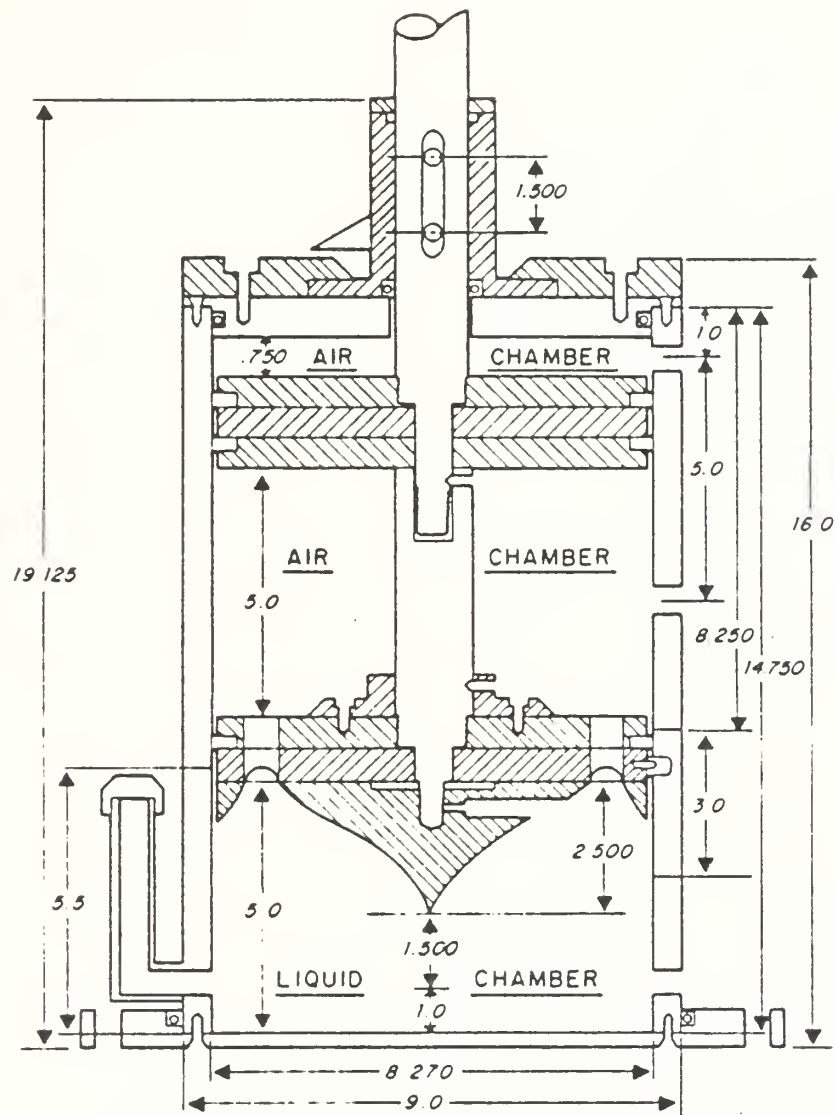


Figure 2. Schematic drawing of the vertical water tunnel.





(dimensions in inch, 1 inch = 2.54 cm)

Figure 3. Valve assembly.





vertical line and with a spacing  $\ell$ . The acceleration was calculated from the fact that the measured differential pressure  $\Delta p$  and the acceleration are related by

$$\rho \ell \frac{dU}{dt} = \Delta p \quad (1)$$

in which  $\rho$  is the density of water and  $\frac{dU}{dt}$  represents the instantaneous acceleration. Repeated measurements of acceleration have shown that the velocity reaches a constant value within 0.05 sec and the acceleration remains zero thereafter.

The velocity was measured through the use of a variable resistance probe. The change in resistance of an about 150 cm long platinum wire, placed vertically in the tunnel away from the tunnel walls, was recorded by an amplifier recorder assembly together with the drag or lift force. The slope of the elevation versus time curve yielded the velocity of the fluid motion through the use of the calibration data.

### C. TEST BODIES AND FORCE MEASUREMENTS

Two smooth aluminum circular cylinders, 60.6 cm long with diameters 62.23 mm and 75.82 mm, respectively, were used in the experiments. The cylinders were turned on a lathe from aluminum pipes. The length of each cylinder was such that it allowed a gap of about 2 mm between the tunnel wall and each end of the cylinder. The cylinder was prevented from moving towards one or the other wall by means of small O-rings attached to the round cantilever end of the force transducers. A double-ball precision bearing was inserted at each end of the cylinder in aluminum housings which sealed the cylinder air tight. The outer face of the bearing was flush with the cylinder.



Two identical force transducers, one at each end of the cylinder, were used to measure the instantaneous drag and lift forces. A special housing was built for each gage so that the gage could be mounted on the tunnel window and rotated to measure either the drag or the lift force alone. The bellows protecting the strain gages were filled with Dow Corning 3140-RTV coating for water proofing. Then the ends of the bellows were sealed air tight.

After mounting one of the cylinders, the exact angular position of each gage within its housing was determined by hanging a load on the cylinder and rotating the gage until the lift force component became zero. The final positions of the gages were marked with a pin. Finally, four bolts were placed on the gage housing to hold the gage rigidly in position. The removal of these bolts and the set pin allowed the rotation of the gage exactly 90 degrees to measure the drag force. Thus, both gages were capable of measuring either one or the other component of total resistance. Usually, one gage was set to measure the drag force and the other, the lift force.

The calibration of the gages was accomplished by hanging loads at the midlength of the cylinder after setting both gages to sense only the drag component. The calibration was also checked by filling the tunnel with water and recording the signal generated by the buoyant force. This procedure provided an easy check on calibration and was used prior to each experiment.



#### IV. DISCUSSION OF RESULTS

The analog data for both the lift and drag forces were evaluated through the use of the calibration constants and plotted in terms of the normalized distance  $Ut/c$  where  $U$  represents the velocity of the steady flow;  $t$ , the time from the start of the motion; and  $c$ , the radius of the cylinder. The drag and lift coefficients were defined as follows:

$$C_D = \frac{\text{Drag Force}}{\frac{1}{2} \rho L D U^2} \quad (2)$$

and

$$C_L = \frac{\text{Lift Force}}{\frac{1}{2} \rho L D U^2} \quad (3)$$

in which  $\rho$  represents the density of water;  $L$ , the length of the cylinder; and  $D$ , the diameter of the cylinder.

##### A. DRAG COEFFICIENT

Figures 4 and 8 show the drag coefficient as a function of  $Ut/c$  for various values of the Reynolds number defined by  $Re = UD/\nu$ . These figures show, regardless of the Reynolds number, that the drag coefficient always rises rapidly to a value of about 1.55 at  $Ut/c$  values from 4 to about 5 and then drops rapidly. The rate of drop as well as the time at which the drag coefficient reaches a steady state value appears to depend on the Reynolds number. At relatively lower



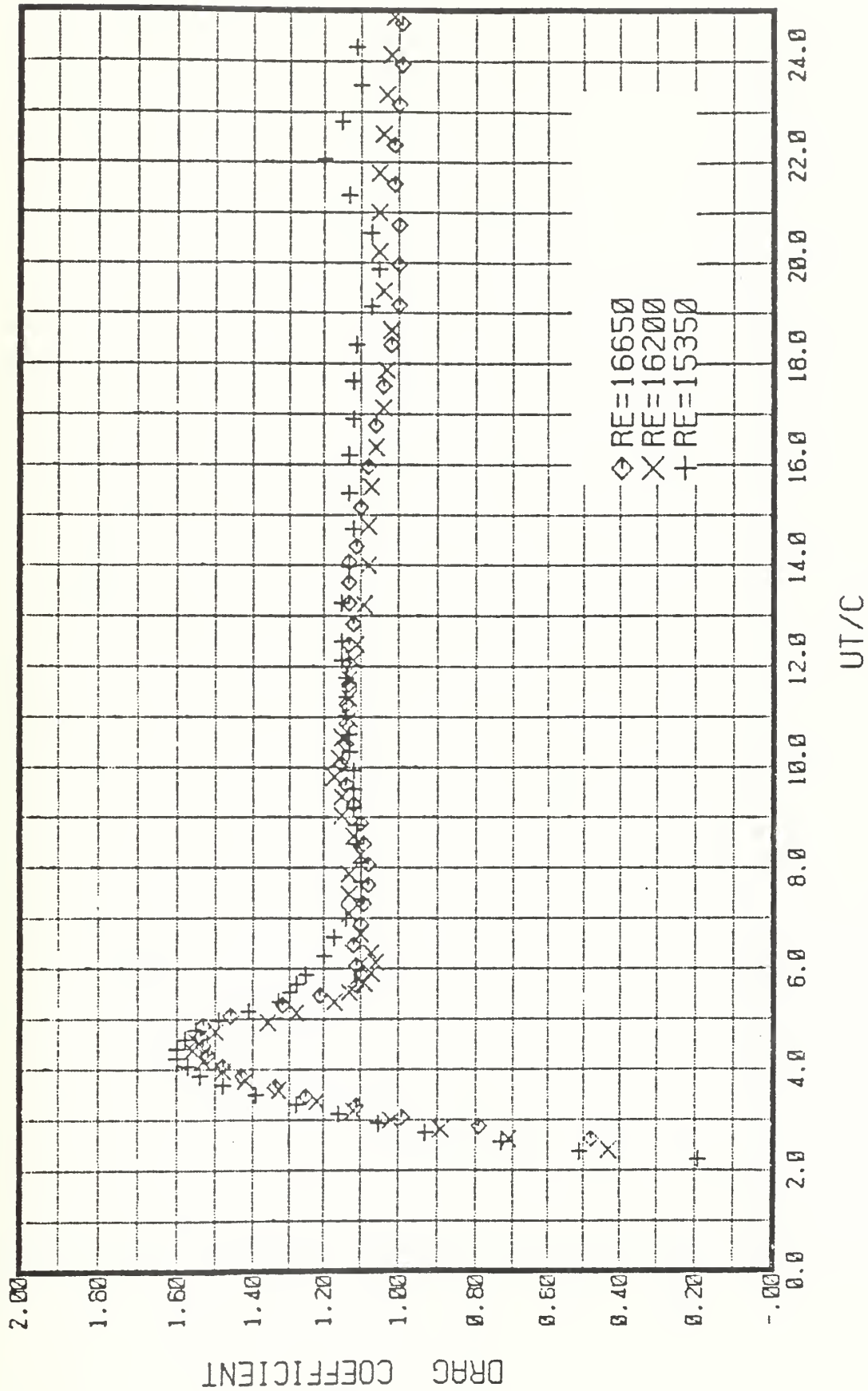


Figure 4.  $C_D$  vs  $U_T/c$  for Reynolds numbers 15,350, 16,200, and 16,650.





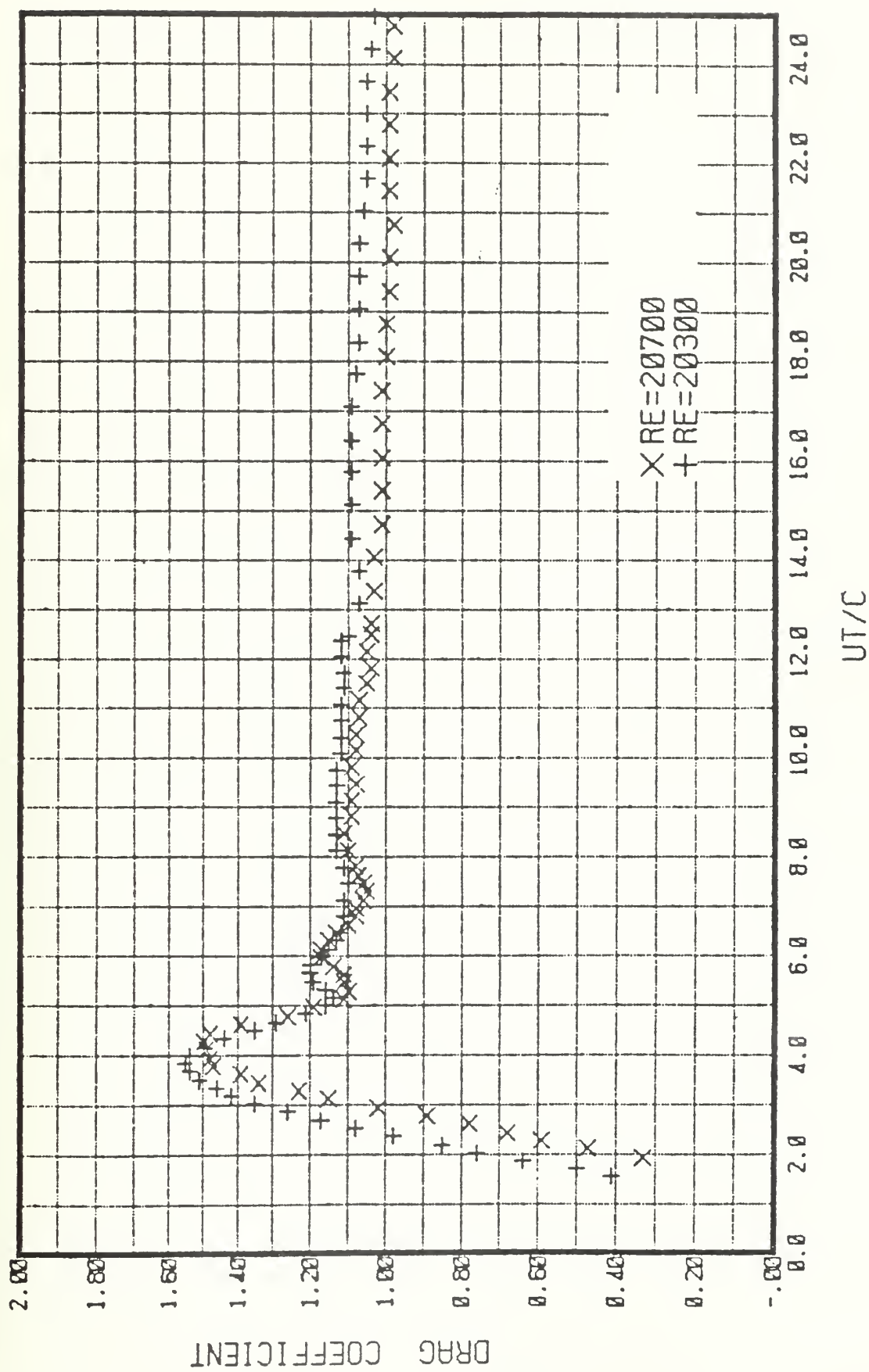


Figure 5.  $C_D$  vs  $Ut/c$  for Reynolds numbers 20,300 and 20,700.



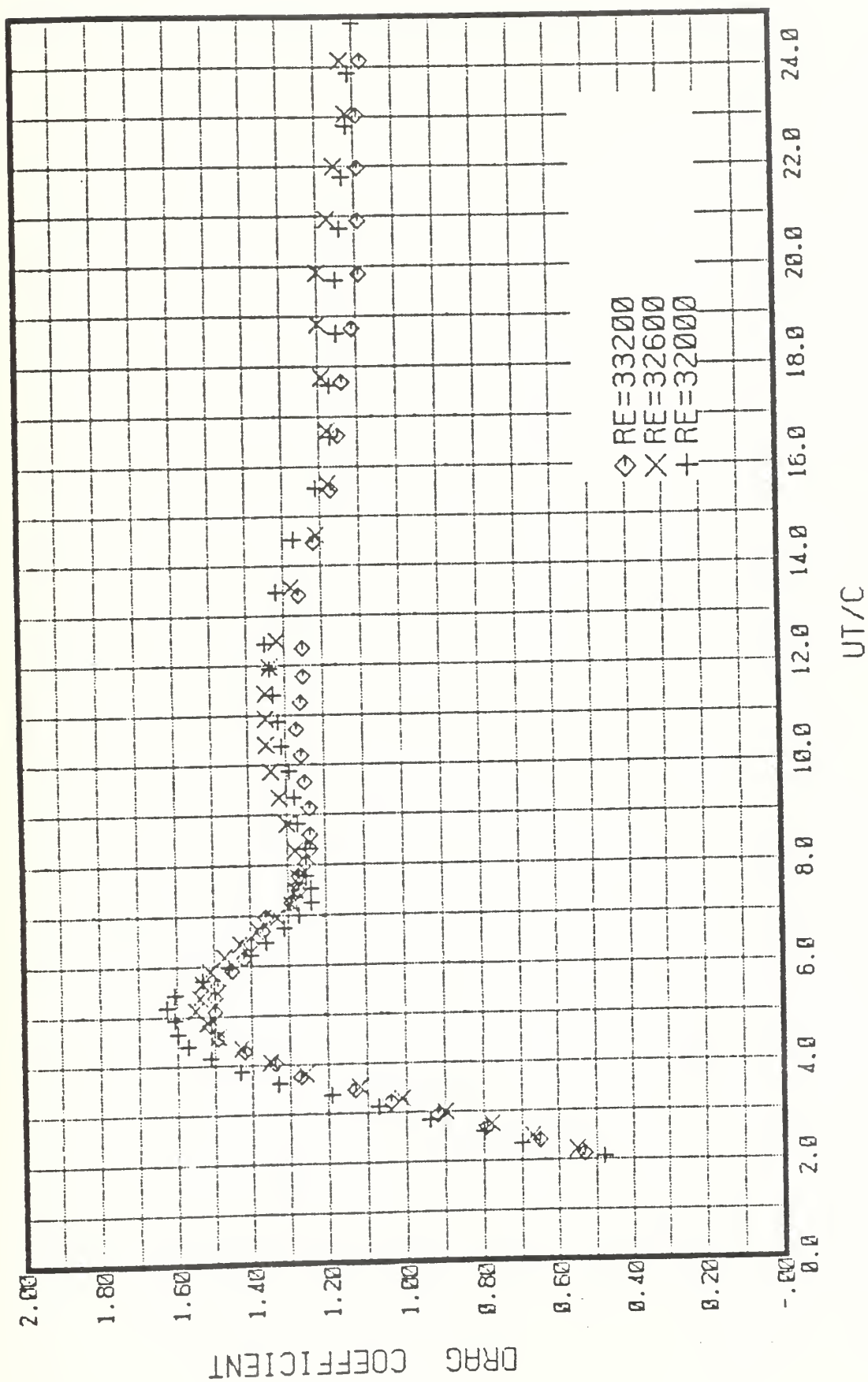


Figure 6.  $C_D$  vs  $UT/c$  for Reynolds numbers 32,000, 32,600, and 33,200.



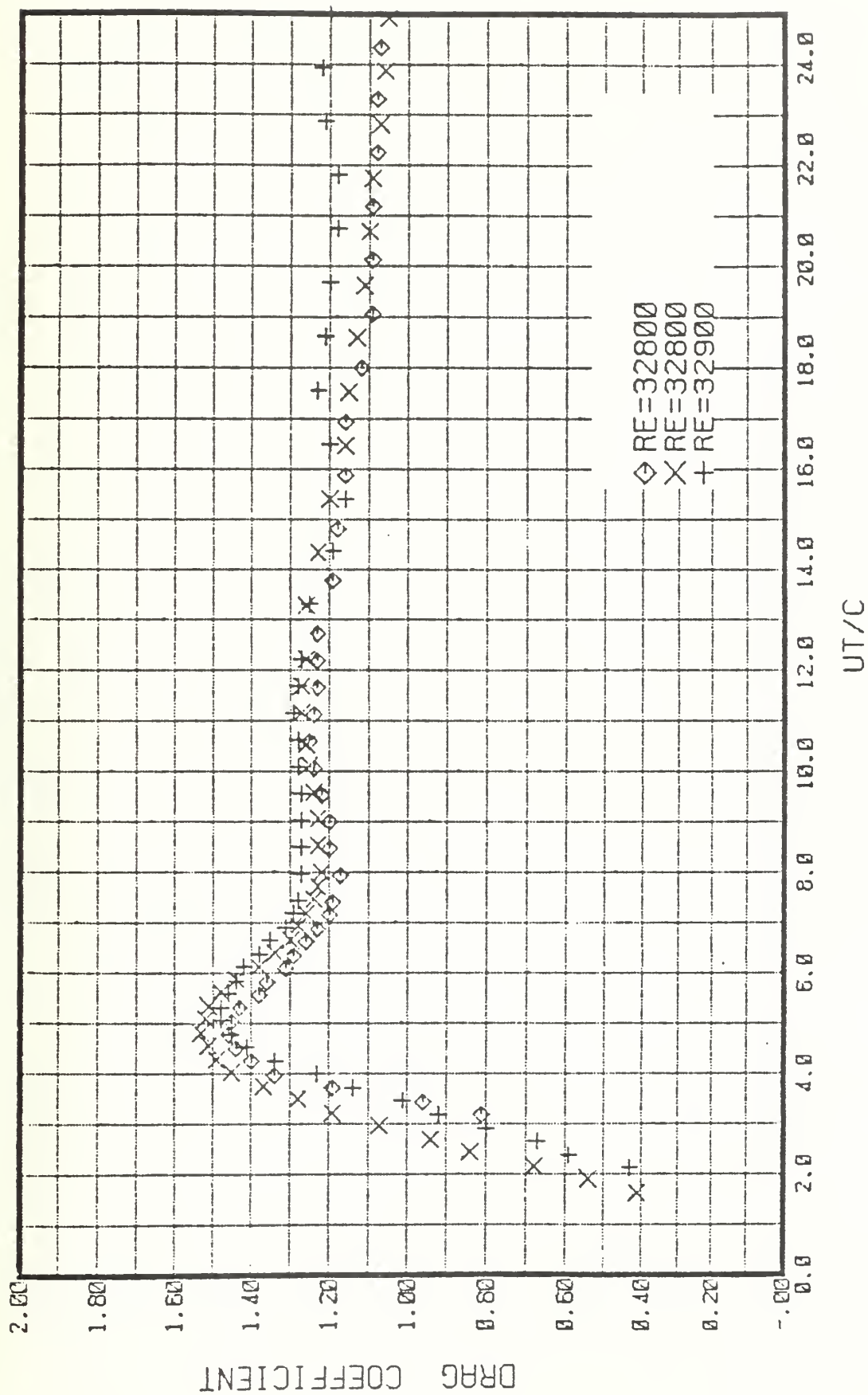
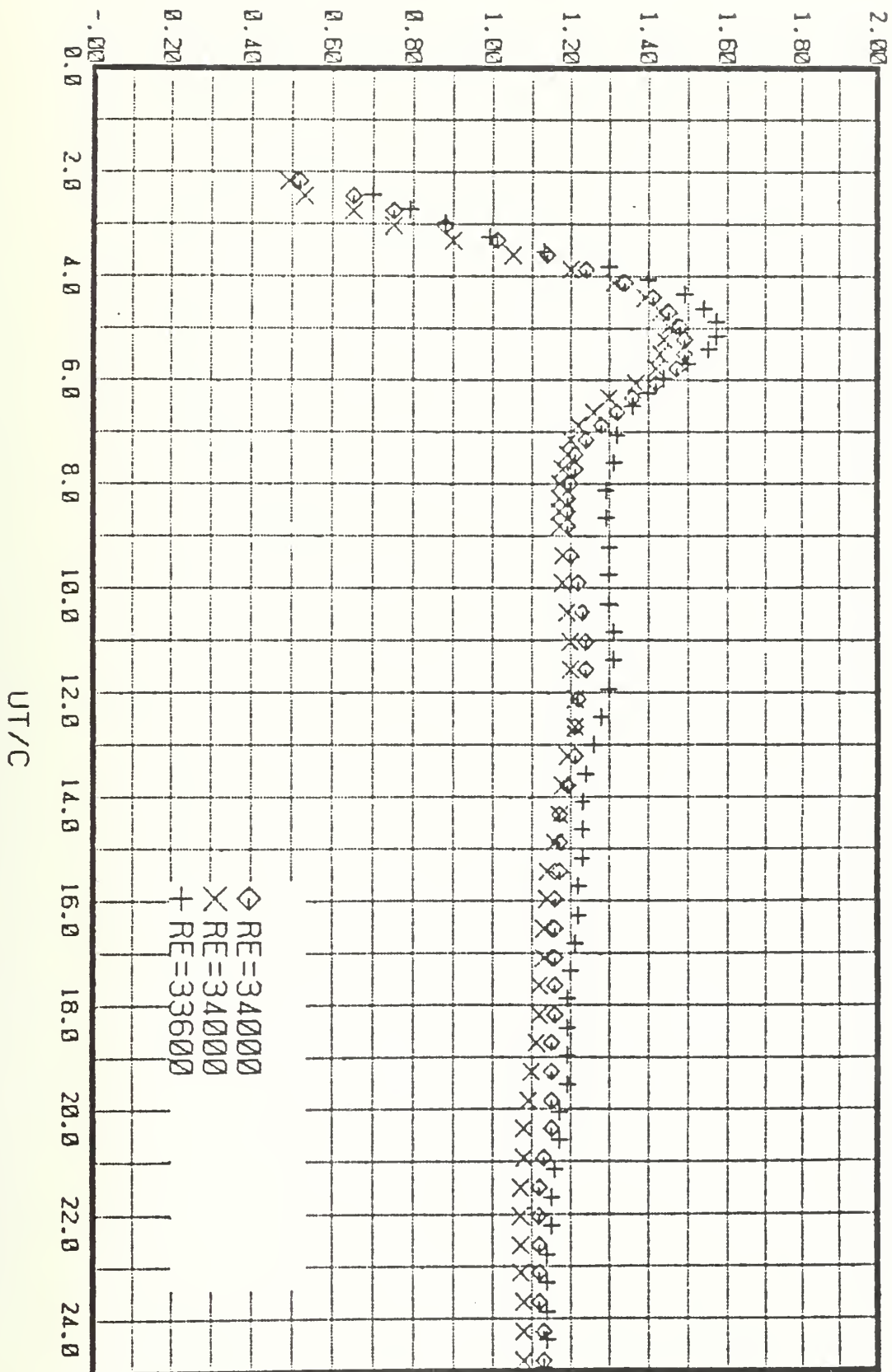


Figure 7.  $C_D$  vs  $Ut/c$  for Reynolds numbers 32,900 and 32,800 (two runs).



# DRAG COEFFICIENT







Reynolds numbers ( $Re = 17,000$ ), the drag coefficient drops to its steady state value at about  $Ut/c = 7$  and thereafter fluctuates about  $C_D = 1.1$  as a result of the lift-induced drag force oscillations. At relatively higher Reynolds numbers ( $Re = 33,000$ ), the maximum peak in the drag coefficient occurs at  $Ut/c = 5$ ; and its value is slightly lower than that for the lower Reynolds numbers. One of the most significant differences between the evolution of the drag coefficient for the smaller and larger Reynolds numbers is in the manner whereby the drag coefficient reaches its steady state value. As noted earlier, at lower Reynolds numbers  $C_D$  rapidly attains its steady state value at about  $Ut/c = 7$ . At higher Reynolds numbers, however,  $C_D$  first decreases from its peak value to a new plateau between 1.25 and 1.3 for  $Ut/c$  values from 7 to 13 and then decreases once more to its steady state value.

The foregoing discussion covered only the general characteristics of the evolution of the drag coefficient with time without making an attempt to explain the reasons giving rise to them. The present experiments as well as those previously conducted by Sarpkaya [3] show that during the initial and symmetric development of vortices (as evidenced by the absence of lift force as will be discussed later) the vorticity rapidly accumulates in the wake. The symmetric vortices grow to sizes considerably larger than those which would be found in the later stages of the motion where the vortices shed alternately. The accumulation of vorticity reduces the back pressure and gives rise to a drag coefficient of about 40% larger than its steady state value. In other words, the initial rise in the drag coefficient is a consequence of the symmetry of the vortices and the accumulation of



of vorticity during this symmetric growth. Once the vortices become asymmetrical under the influence of ever present small disturbances, one vortex moves away from the cylinder causing a rapid drop in the drag force and a gradual increase in the lift force. Evidently the rate of rise and the peak value of the drag coefficient are not materially affected by the disturbances since the vortices continue to retain their symmetry for  $Ut/c$  values smaller than about 5. It is possible to show that the vortices must acquire certain strength and position relative to the cylinder in order to reach a state at which they are most susceptible to disturbances. Once the vortices begin to shed, the drag coefficient reaches a value of about 1.1, a value which is commonly accepted at the Reynolds numbers encountered herein.

The peak value of the drag coefficient, its time of occurrence, and subsequent decrease to steady state values are also related to the character of the fluid motion (laminar or turbulent), and hence on the dissipation of circulation. It is a well known fact that the fluid motion in the near wake is turbulent for Reynolds numbers larger than about 200. The rate of decrease of circulation in each vortex depends on the intensity of turbulence and hence on the Reynolds number. Numerical analysis through the use of discrete vortices [3] has shown that the larger the dissipation, the smaller is the peak value of  $C_D$  and the more gradual is the decrease of  $C_D$  to its steady state value. Evidently, a vortex pair of smaller circulation gives rise to a smaller drag coefficient since  $C_D$  is proportional to the square of  $\Gamma/Uc$ . The experimental results reported herein are in conformity with the foregoing conjectures. At higher Reynolds numbers ( $Re \approx 33,000$ ) the peak value of  $C_D$  is about 1.5 and occurs at a  $Ut/c$  value closer to 5, in



contrast to a  $C_D$ -value of 1.55 at  $Ut/c \approx 4$  for Reynolds numbers of about 16,000. The dissipation of vorticity evidently requires that the symmetric vortices be fed a relatively longer time period [ $\Delta(Ut/c) \approx 1$ ] in order to allow the vortices to reach their maximum strength. As noted earlier the vortices gradually become asymmetrical and a turbulent vortex, being inherently more stable to disturbances relative to the one at lower Reynolds numbers, lingers somewhat longer in the vicinity of the cylinder. These ideas have previously been substantiated through measurements and flow visualization by Sarpkaya [3]. The extended stay of the vortices in the vicinity of the cylinder does not allow the drag force to drop rapidly to its steady state value. Suffice it to note that the evolution of the drag force with time depends on the Reynolds number. The larger the Reynolds number, the larger is the dissipation of vorticity, and the smaller the peak value of  $C_D$ . It has been noted previously that there is a plateau in  $C_D$  for  $Ut/c$  values between 7 and 13 for larger Reynolds numbers. It is now clear that that plateau is a consequence of the dissipation of circulation in the vortices. It is also clear that one must further substantiate these ideas by carrying out experiments at even higher Reynolds numbers.

## B. LIFT COEFFICIENT

The lift coefficient versus  $Ut/c$  plots are presented in Figs. 9 through 12 for various values of the Reynolds number. The Reynolds numbers in these plots do not exactly correspond to those in the drag coefficient plots because of the fact that the lift and drag force runs were carried out independently. It was not possible to record simultaneously the elevation and the lift and drag forces because of the lack of a high-speed three-channel recorder.



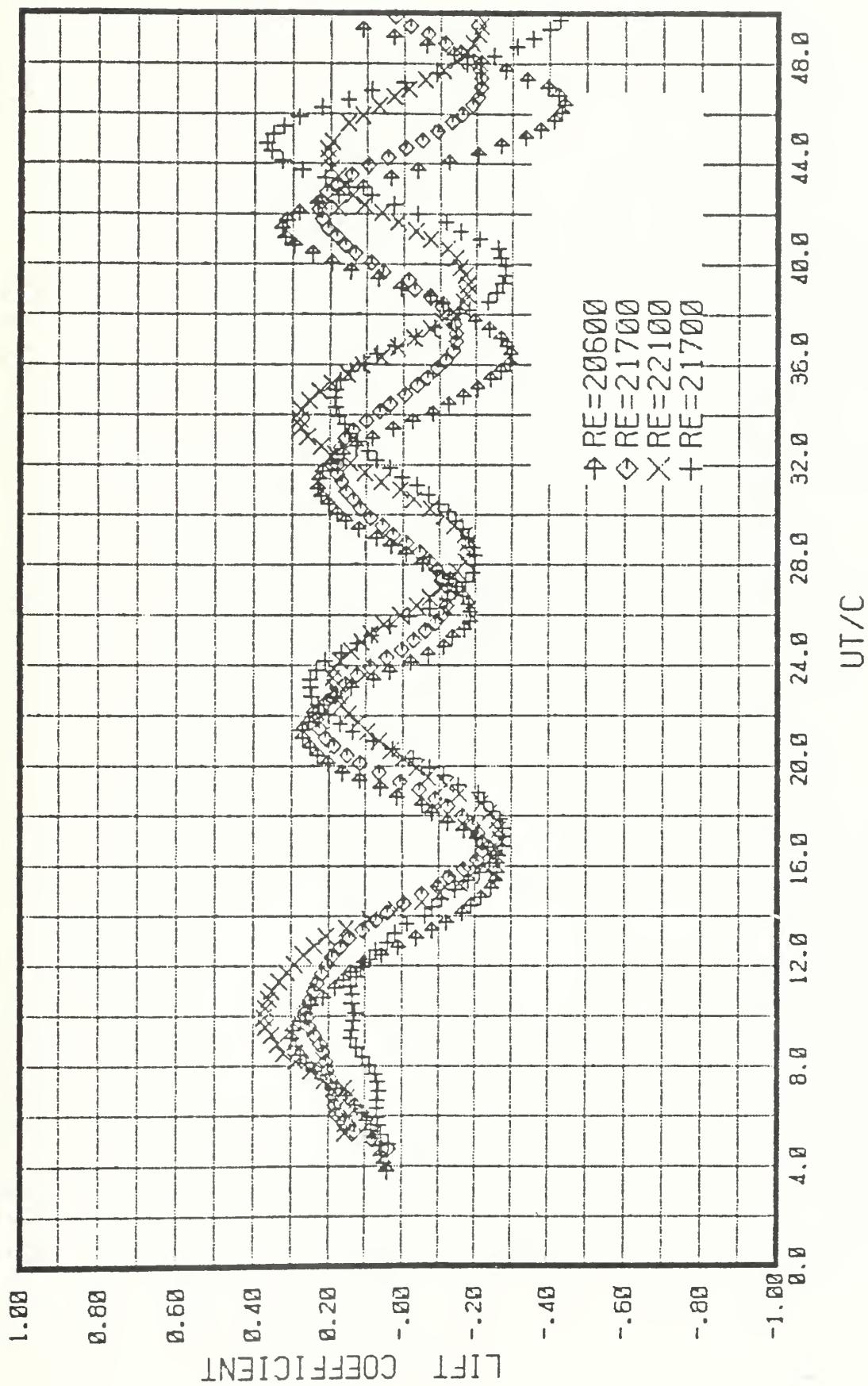


Figure 9.  $C_L$  vs  $Ut/c$  for Reynolds numbers 20,600, 22,100, and 21,700 (two runs).





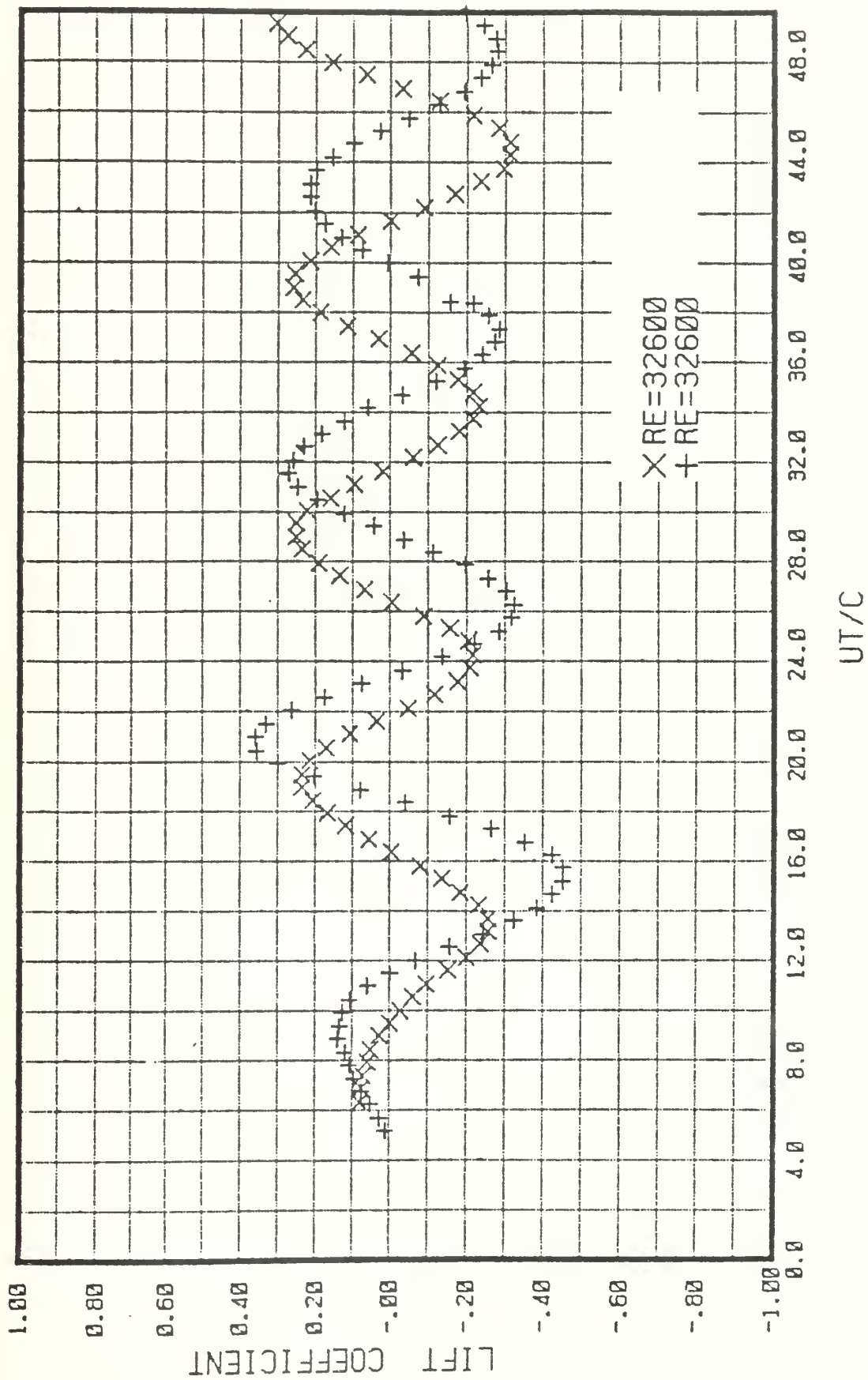


Figure 10.  $C_L$  vs  $Ut/c$  for Reynolds number 32,600 (two runs).



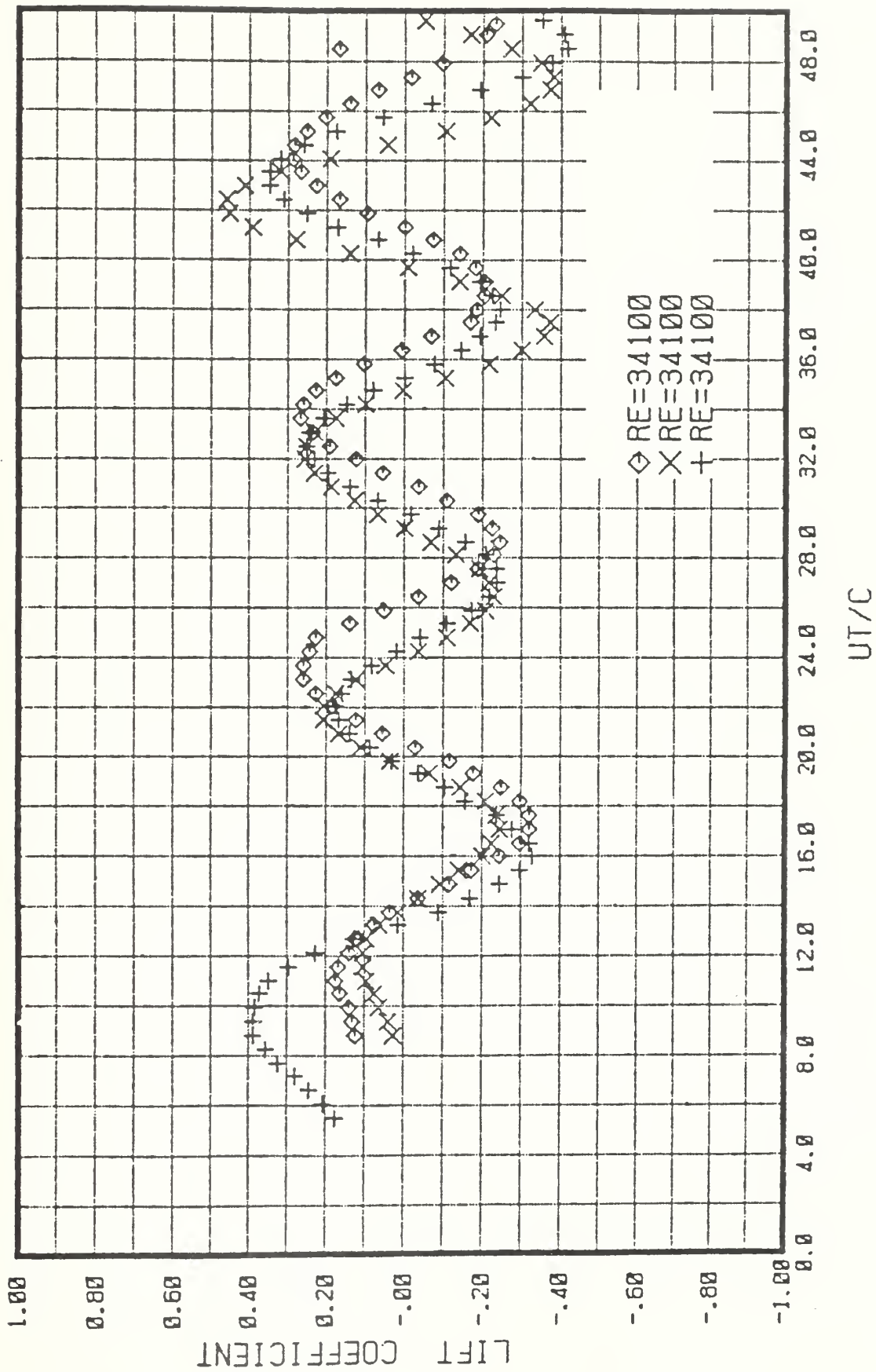


Figure 11.  $C_L$  vs  $UT/c$  for Reynolds number 34,100 (three runs).



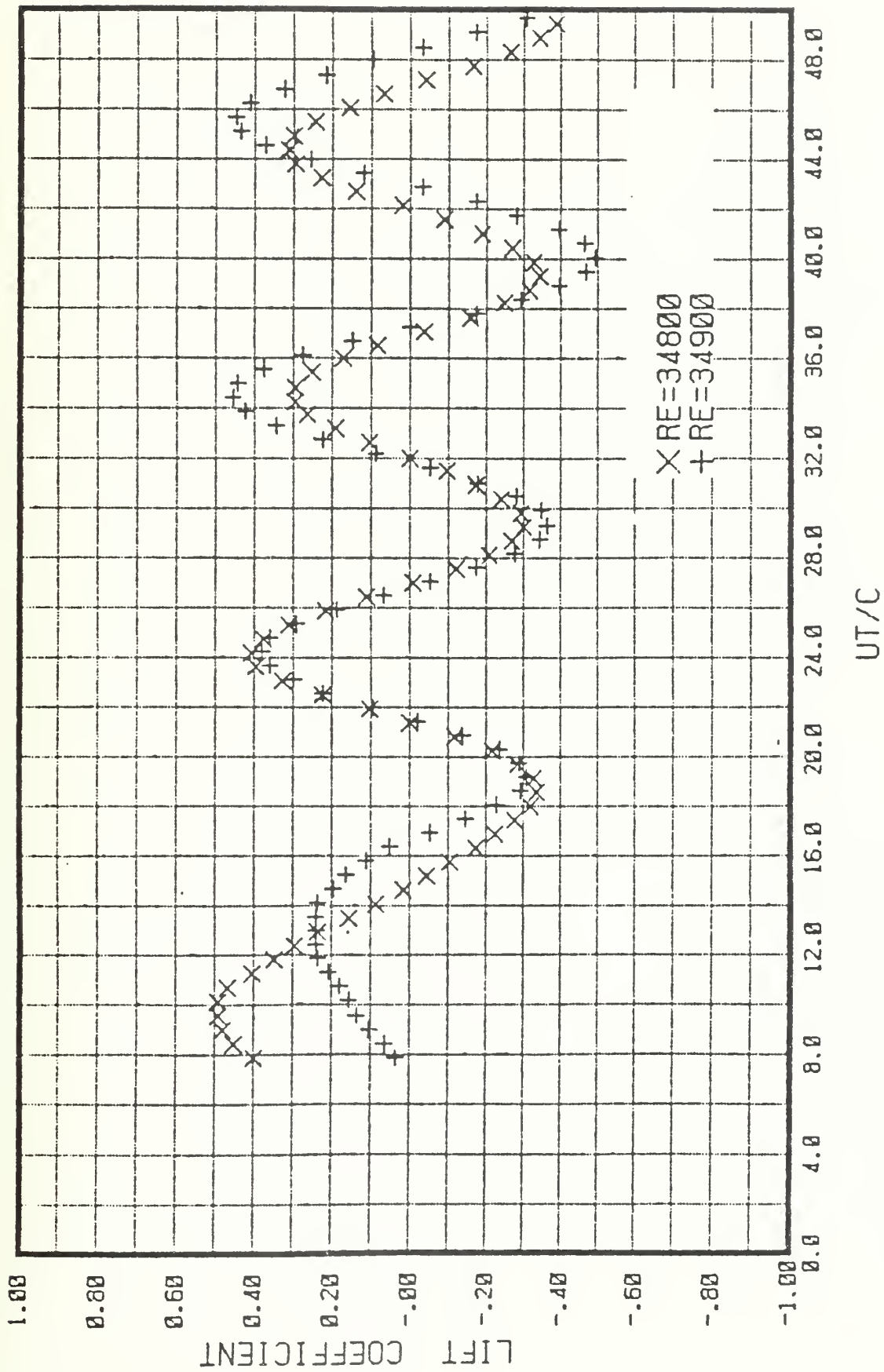


Figure 12.  $C_L$  vs  $U_T/c$  for Reynolds numbers 34,800 and 34,900.



A quick examination of the lift plots show that the lift force remains practically zero until the vortices become asymmetrical at  $Ut/c$  values of about 6, the amplitude of the lift force varies significantly from one run to another even for identical Reynolds numbers, and the first few peaks of the alternating lift force do not occur at the same  $Ut/c$  values. In general, however, the lift coefficient reaches a maximum value of about 0.4. This value is in conformity with those obtained previously in steady flows at the corresponding Reynolds numbers [14].

There are various reasons for the observed behavior of the lift force. Firstly, even in steady flows the lift coefficient shows large variations at a given Reynolds number for all Reynolds numbers. This is primarily because of the inherent instability of the vortices, the surface condition and length-to-diameter ratio of the cylinder, and the lack of spanwise coherence of the vortex cores. Secondly, in impulsive flow the development of lift is strongly dependent on the initial disturbances which give rise to asymmetry and subsequent vortex shedding. Consequently, it is not too surprising to find that in some runs the vortices continue to grow symmetrically and thus result in very small lift forces. In some runs asymmetry develops rapidly and the lift force not only starts at smaller values of  $Ut/c$  but also reaches larger amplitudes. Since there is no way to control the magnitude of the disturbances, other than assuring that the fluid in the tunnel is as quiescent as possible prior to each run, one must anticipate relatively large variations both in the magnitude and the time of occurrence of the peak values of lift. Suffice it to note that the lift force is a fairly random quantity and that randomness is certainly reflected in the data presented herein. The data further helps to





explain the random nature of the side forces measured on missile models mounted in wind tunnels. It appears that attempts to obtain a unique lift-force variation will not be fruitful in view of the stated randomness of the lift forces.



## V. CONCLUSIONS

The experimental investigation of the impulsively-started flow about smooth circular cylinders in a vertical water tunnel warranted the following conclusions:

1. The drag coefficient reaches a peak value of 1.5 to 1.55, depending on the Reynolds number, at  $Ut/c$  values from about 4 to 5;

2. the drag coefficient eventually drops to its steady state value for  $Ut/c$  larger than about 7;

3. the lift coefficient begins to develop at  $Ut/c$  values larger than about 6 and alternates about a zero mean value with an amplitude of about 0.4. The magnitude and the time of occurrence of the peak values are strongly dependent on the magnitude and distribution of the initial disturbances;

4. the lift and drag coefficients both appear to depend on the Reynolds number. Only additional experiments at higher Reynolds numbers could determine the extent and form of the dependence on the Reynolds number.



## LIST OF REFERENCES

1. Munk, M. M., "The Aerodynamic Forces on Airship Hulls," NACA Technical Report No. 184; Annual Reports, 9, 1923.
2. Allen, H. J. and Perkins, E. W., "A Study of Effects of Viscosity on Flow Over Slender Inclined Body of Revolution," NASA Report No. 1048, 1951.
3. Sarpkaya, T., "Separated Flow about Lifting Bodies and Impulsive Flow about Cylinders," AIAA Journal, Vol. 4, No. 3, 1966, p. 414-422.
4. Kelly, H. R., "The Estimation of Normal-Force, Drag, and Pitching-Moment Coefficients for Blunt-Based Bodies of Revolution at Large Angles of Attack," Journal of the Aeronautical Sciences, Vol. 21, No. 8, 1954, pp. 549-555, 565.
5. Hill, J. A. F., "A Non-Linear Theory of the Lift on Slender Bodies of Revolution," NavOrd Report 5338, 1954.
6. Bryson, A. E., "Symmetric Vortex Separation on Circular Cylinders and Cones," Journal of Applied Mechanics, Vol. 26, 1959, pp. 643-648.
7. Blasius, H., "Grenzschichten in Flüssigkeiten mit kleiner Reibung," Z. Math. u. Phys., Vol. 56, No. 1, 1908.
8. Rosenhead, L., "Formation of Vortices from a Surface of Discontinuity," Proceedings of the Royal Society of London, Vol. A-134, 1931, pp. 170-192.
9. Görtler, H., "Grenzschichtentstehung an Zylindern bei Anfahrt aus der Ruhe," Archive der Math., Vol. 1, 1948, pp. 138-147.
10. Schuh, H., "Über die 'ähnlichen' Lösungen der instationären laminaren Grenzschichtgleichungen in inkompressibler Strömung," "Fifty Years of Boundary-Layer Research," Braunschweig, 1955, pp. 147-152.
11. Watson, J., "A Solution of the Navier-Stokes Equations, Illustrating the Response of a Laminar Boundary Layer to a Given Change in the External Stream Velocity," Quarterly Journal of Mechanics and Applied Mathematics, Vol. 11, 1958, pp. 302-325.
12. Wundt, H., "Wachstum der laminaren Grenzschicht an schräg angeströmten Zylindern bei Anfahrt aus der Ruhe," Ing.-Arch., Vol. 23, 1955, pp. 212-230.



13. Schwabe, M., "Über Druckermittlung in der instationären ebenen Strömung," Ing.-Arch., Vol. 6, 1935, pp. 34-50; NACA TM 1039, 1943.
14. Lienhard, J. H., "Synopsis of Lift, Drag, and Vortex Frequency Data for Rigid Circular Cylinders," Bulletin No. 300, Washington State University, College of Engineering, Pullman, Washington, 1966.





# INITIAL DISTRIBUTION LIST

	<u>No. Copies</u>
1. Defense Documentation Center Cameron Station Alexandria, Virginia 22314	2
2. Library, Code 0142 Naval Postgraduate School Monterey, California 93940	2
3. Department Chairman, Code 69 Mechanical Engineering Naval Postgraduate School Monterey, Calif. 93940	1
4. Office of Naval Research 800 N. Quincy Street Arlington, VA 22217	1
5. Office of Naval Research Branch Office 495 Summer Street Boston, MA 02210	1
6. National Science Foundation Washington, D. C. 20550 Attn: Dr. G. K. Lea	20
7. Naval Weapons Center China Lake, CA 93555	1
8. Library of Congress Science & Technology Division Washington D. C. 20540	1
9. Prof. T. Sarpkaya Mechanical Engineering Naval Postgraduate School Monterey, CA 93940	5
10. Dean of Research, Code 012 Naval Postgraduate School Monterey, Calif. 93940	1

DUDLEY KNOX LIBRARY



3 2768 00335507 4